SJR SCImago Journal & Country Rank

EST MODUS IN REBUS

Home
Journal Rankings
Journal Search
Country Rankings
Country Search
Compare
Map Generator
Help
About Us

Show this information in your own website

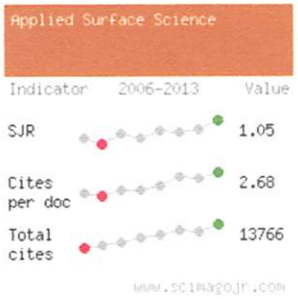

Display journal title

Just copy the code below and paste within your html page:

<a href="http://www.scimagojr.

Related product

SCIMAGO INSTITUTIONS RANKINGS

@scimago

SJR is developed by:

Scimago Lab

Journal Search

Search query

in Journal Title Search

Exact phrase

Applied Surface Science

Country: Netherlands

Subject Area: Materials Science

Subject Category:

Category	Quartile (Q1 means highest values and Q4 lowest values)														
	1999	2000	2001	2002	2003	2004	2005	2006	2007	2008	2009	2010	2011	2012	2013
Surfaces, Coatings and Films	Q1	Q1	Q1	Q1	Q1	Q1	Q1	Q1	Q1	Q1	Q1	Q1	Q1	Q1	Q1

Publisher: Elsevier. **Publication type:** Journals. **ISSN:** 01694332

Coverage: 1984-2014

H Index: 103

Scope:

Applied Surface Science covers topics contributing to a better understanding of applications of surfaces, interfaces, thin films and other nanostructures. [...]
Show full scope

Charts Data

SJR indicator vs. Cites per Doc (2y)

Flash out-of-date

The SJR indicator measures the scientific influence of the average article in a journal, it expresses how central to the global scientific discussion an average article of the journal is. Cites per Doc. (2y) measures the scientific impact of an average article published in the journal, it is computed using the same formula that journal impact factor ™ (Thomson Reuters).

Citation vs. Self-Citation

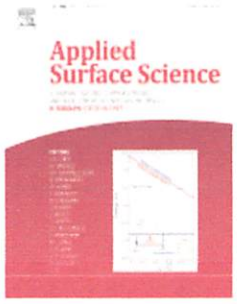

Supports Open Access

Applied Surface Science

A Journal Devoted to Applied Physics and Chemistry of Surfaces and Interfaces

Applied Surface Science covers topics contributing to a better understanding of applications of **surfaces**, **interfaces**, and **nanostructures**. The journal is concerned with scientific research on the atomic...

View full aims and scope

Editor-in-Chief: H. Rudolph
View full editorial board

Guide for Authors
Submit Your Paper
Track Your Paper
Order Journal
View Articles

Journal Metrics

Source Normalized Impact per Paper (SNIP): 1.531

SCImago Journal Rank (SJR): 1.045

Impact Factor: 2.538

5-Year Impact Factor: 2.469

Imprint: NORTH-HOLLAND

ISSN: 0169-4332

Stay up-to-date

Register your interests and receive email alerts tailored to your needs

Click here to sign up

Follow us

Subscribe to RSS

Latest News

News

Frans Habraken Best Paper Award
Submission deadline is March 1st, 2015

Meet the Winner of the Prize Draw at AVS 2014

Dan Zhang receives Frans Habraken Award at CPS, Harbin, China

VIEW ALL

Recent Open Access Articles

Ambient pressure photoemission spectroscopy of metal surfaces
Iain D. Baikie | Angela C. Grain | ...

Triple-junction InGaP/GaAs/Ge solar cells integrated with polymethyl methacrylate subwavelength structure
Dae-Seon Kim | Yonkil Jeong | ...

Plasma electrolytic oxidation of titanium in a phosphate/silicate electrolyte and tribological performance of the coatings
S. Aliasghari | P. Skeldon | ...

VIEW ALL

Recent Articles

Most Downloaded Articles

1. The effect of heat treatment on the physical properties of sol–gel derived ZnO thin films
Davood Raoufi | Taha Raoufi

2. In situ green synthesis of silver–graphene oxide nanocomposites by using tryptophan as a reducing and stabilizing agent and their application in SERS
Biwen Yang | Zhiming Liu | ...

3. Effect of deposition variables on properties of CBD ZnS thin films prepared in chemical bath of ZnSO4/SC(NH2)2/Na3C3H5O7/NH4OH
Wei-Long Liu | Chang-Siao Yang | ...

VIEW ALL

Journal Insights

Discover this journal's metrics

FIND OUT MORE

Applied Surface Science 311 (2014) 54–61

Contents lists available at ScienceDirect

Applied Surface Science

journal homepage: www.elsevier.com/locate/apsusc

Hydroxyapatite electrodeposition on anodized titanium nanotubes for orthopedic applications

Yardnapar Parcharoen[a], Puangrat Kajitvichyanukul[b], Sirinrath Sirivisoot[a], Preecha Termsuksawad[c,*]

[a] Department of Biological Engineering, Faculty of Engineering, King Mongkut's University of Technology Thonburi, Bangkok, Thailand
[b] Center of Excellence on Environmental Research and Innovation, Faculty of Engineering, Naresuan University, Phitsanulok, Thailand
[c] Division of Materials Technology, School of Energy, Environment and Materials, King Mongkut's University of Technology Thonburi, 126 Pracha Uthit Rd., Bang Mod, ThungKhru, Bangkok 10140, Thailand

ARTICLE INFO

Article history:
Received 7 January 2014
Received in revised form 21 April 2014
Accepted 30 April 2014
Available online 9 May 2014

Keywords:
TiO_2 nanotubes
Anodic oxidation
Medium modifiers
Orthopedic implants

ABSTRACT

Nanotubes modification for orthopedic implants has shown interesting biological performances (such as improving cell adhesion, cell differentiation, and enhancing osseointegration). The purpose of this study is to investigate effect of titanium dioxide (TiO_2) nanotube feature on performance of hydroxyapatite-coated titanium (Ti) bone implants. TiO_2 nanotubes were prepared by anodization using ammonium fluoride electrolyte (NH_4F) with and without modifiers (PEG400 and Glycerol) at various potential forms, and times. After anodization, the nanotubes were subsequently annealed. TiO_2 nanotubes were characterized by scanning electron microscope and X-ray diffractometer. The amorphous to anatase transformation due to annealing was observed. Smooth and highly organized TiO_2 nanotubes were found when high viscous electrolyte, NH_4F in glycerol, was used. Negative voltage (−4 V) during anodization was confirmed to increase nanotube thickness. Length of the TiO_2 nanotubes was significantly increased by times. The TiO_2 nanotube was electrodeposited with hydroxyapatite (HA) and its adhesion was estimated by adhesive tape test. The result showed that nanotubes with the tube length of 560 nm showed excellent adhesion. The coated HA were tested for biological test by live/dead cell straining. HA coated on TiO_2 nanotubes showed higher cells density, higher live cells, and more spreading of MC3T3-E1 cells than that growing on titanium plate surface.

1. Introduction

Biomaterials are artificial or natural materials used to replace the lost or infected biological structure. Commonly-used biomaterials for orthopedic implants are 316L stainless steels, cobalt–chromium alloys, and titanium and its alloys. Among these materials, titanium is preferred for orthopedic implants because it possesses closer elastic modulus to that of bone than other [1,2]. However, using titanium as bone implant often fails after long-term use due to an incomplete osseointegration (incomplete bonding between the implant and surrounding bone) [3,4]. Surface treatments such as roughening by sand blasting, formation of anatase phase TiO_2 [5], hydroxyapatite coating, or chemical treatment [6–10] have been used to improve bioactivity of titanium and to enhance bone growth. Webster et al. reported that nano-grained ceramics (with surface structures less than 100 nm) can improve bioactivity of titanium implants and enhance osteoblast adhesion [11,12]. In this aspect, nanoscaled modification is an alternative to improve osseointegration of titanium-based orthopedic implants [13,14]. Therefore, nanotubular TiO_2 arrays are highly interested in this study because of its nanoscale and high surface area.

Titanium oxide nanotubes can be prepared by various techniques, such as sol–gel method [15], electrophoretic deposition [16] and anodization [17]. Among these methods, fabrication of vertically aligned TiO_2 nanotubes on titanium substrate could be easily obtained by anodization [17]. Various researchers prepared the nanotubular structures by electrochemical anodization in hydrofluoric acid containing electrolytes [18,19]. However, to be non-toxic and environment friendly, neutral fluoride solution (NH_4F) was used as the electrolyte in this work. Metal oxide formation and nanotube self-assembly are formed by carefully balancing between the electrochemical processes (field-assisted oxide growth and metal etching) and chemical dissolution of the substrate (the presence of an acidic or complex-forming electrolyte)

* Corresponding author. Tel.: +66-2470-8695-9x302; fax: +66-2470-8643.
E-mail address: preecha.ter@kmutt.ac.th (P. Termsuksawad).

http://dx.doi.org/10.1016/j.apsusc.2014.04.207
0169-4332/

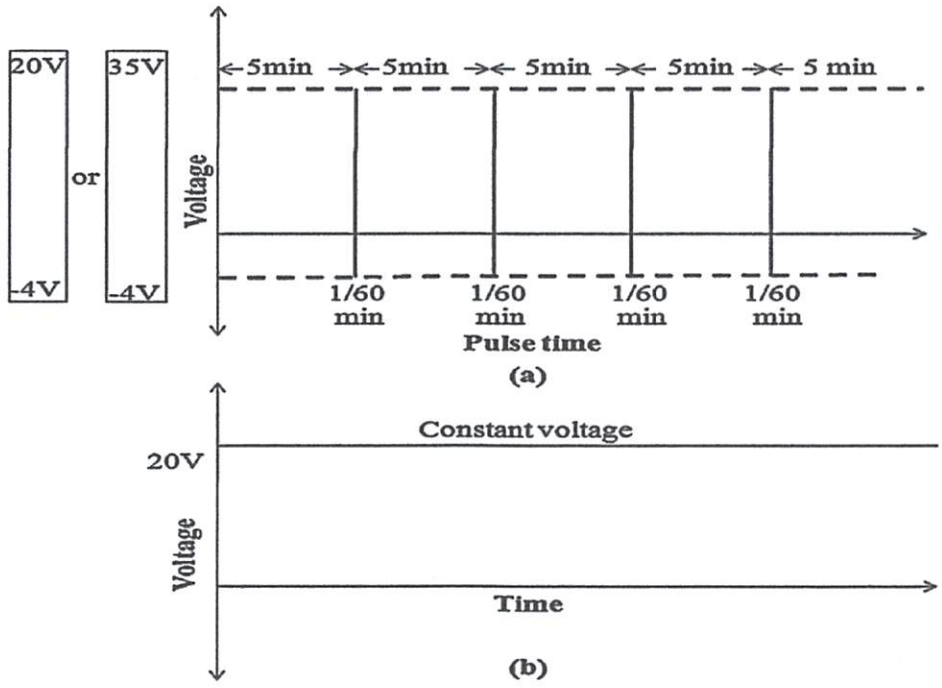

Fig. 1. Potential pulse waveform (a) and constant potential (b) used for anodic growth of TiO_2 nanotube arrays.

[20,21]. To obtain this balance, pulse anodization was used to control chemical dissolution [22]. In the other works, micrometer-long TiO_2 nanotubes with uniform or smooth tube walls were formed when high viscous electrolytes containing fluoride ions were used [23,24]. Therefore, to achieve uniform and well oriented TiO_2 nanotube array, pulse anodization and viscous electrolyte were used in this study.

Another approach to enhance osseointegration of Ti implants is coating titanium with nanostructured hydroxyapatite (HA) (main mineral in bones with the molar Ca/P ratio of 1.67 in stoichiometric hydroxyl apatite ($Ca_{10}(PO_4)_6(OH)_2$)[25]). The HA-coated titanium was shown to have excellent corrosion resistance and good biocompatibility [2]. With electrodeposition, HA with complex shapes can be obtained and thickness of coating can be easily controlled at low temperature. In this work, to search for the optimum conditions for fluoride anodization, the growing of TiO_2 nanotube layers in different viscous electrolytes, various times and pulse anodization were studied. Nanostructured HA coatings were electrodeposited on TiO_2 nanotube arrays after anodization and surface alkali treatment, respectively. After that, adhesion of HA electrodepositions coating on the nanotube from each anodization conditions were measured by ASTM D 3359-02: Standard Test Methods for Measuring Adhesion by Tape; cross-cut tape test (B). Finally osteoblast cells behavior on HA coated anodized titanium surface (ATi) was investigated.

2. Experimental

2.1. Preparation of titanium

Titanium plate with 1.0 mm. thickness (Alfa Aesar, 99.2 wt.%) was used as a substrate to grow oxide nanotube arrays. The surface was polished to mirror quality using silicon carbide paper (TOA, Thailand) of successively finer roughness (400, 600, 800, 1000, 1500 and 2000 grits), and following by polishing with 0.05-μm alumina powder (Allied, USA). After polishing, the titanium plate was washed with deionized (DI) water and was sonicated for 5 min in acetone and another 5 min in ethanol.

2.2. Anodization to form TiO_2 nanotube arrays

The titanium nanotube layers were prepared by electrochemical method. Platinum wire and the titanium plate were used as negative and positive electrodes, respectively. All films were grown at approximately 25 °C in 0.36 M ammonium fluoride (NH_4F) electrolytes (viscosity of 0.764 cP) with and without modifiers: 10% (NH_4F in H_2O):90% Glycerol, (viscosity of 300 cP) or polyethylene glycol 400 (viscosity of 133.71 cP). The viscosity of electrolyte was measured by cylinder rotation viscosity technique (Viscometer DV II+ (Brookfield, USA). Anodization was conducted with two different potential forms: pulse (20/−4 V) and constant (20 V) voltage, as shown in Fig. 1. Anodization time was varied as 0.5, 1.5 and 2.5 h. After anodization, samples were carefully cleaned with DI water and then were dried by nitrogen gas. The grown porous layers were annealed at 450 °C for 30 min to obtain anatase phase.

2.3. Electrodeposition of hydroxyapatite

It was reported that HA coating on ATi, anodized titanium, from electrodeposition without any surface treatment was not homogenous [26]. To obtain homogenous HA, the ATi samples were treated by 1 M NaOH solution at 50 °C for 2 min prior to electrodeposition. After the pre-treatment, the HA deposition was conducted. The electrolyte was prepared by dissolving 1.67 mM phosphate containing salt in the form of $NH_4H_2PO_4$ (Sigma, Thailand) and 2.5 mM calcium containing salt in the form of $Ca(NO_3)_2$ (Sigma, Thailand) in distilled water. To increase ionic conductivity, 0.15 M NaCl was dissolved in the electrolyte and the pH of electrolyte was buffered at 7.2 by tris(hydroxyl aminomethane), and hydrochloric acid [26]. The pre-treated ATi and platinum were used as a cathode and an anode, respectively. The electrodeposition of HA was carried out at a constant potential, −2.5 V, at 80 °C for 10 min.

2.4. Morphological and structural characterization

The surface morphology of ATi was investigated by a scanning electron microscopy (FE-SEM, CamScanMX2600) with a nominal

electron beam voltage of 10 kV. The tube diameter, tube length and tube wall thickness were measured by image analysis software (Image J, Montgomery). The crystal structures of ATi before and after annealing were examined by X-ray diffractometer (Bruker D8 Advance) in the range of $2\theta = 5–80°$.

2.5. Adhesive tape test

The adhesion of the HA coating to the substrate was measured using ASTM D 3359-02 cross-cut tape-test (B) [27]. Grid of 6×6 parallel cuts with 1 mm gaps between them was made through the coating down to the substrate. The 3 M Brand Scotch tape was firmly placed in the area of the grid and it was pulled abruptly off at an angle as close to 180° as possible after 90 s. Damage of the coating was evaluated visually by SEM-EDS (FE-SEM, Nova NanoSEM 450, US). The damage area of the samples (expressed in percent) was classified into these scales: 5 = 0%; 4 = less than 5%; 3 = 5–15%; 2 = 15–35%; 1 = 35–65%; 0 = over 65%.

2.6. Calcein AM/Ethidium homodimer-1 staining for live/dead assay

Human osteoblasts (MC3T3-E1, passage number = 4) were used to test for observation of live (green) and dead cells (red). Cells were cultured in Dulbecco's Modified Eagle Medium (DMEM) (In-Vitrogen Corporation) supplemented with 10 vol.% of fetal calf serum (Dominique Dutcher), and 1 vol.% of penicillin/streptomycin (In-Vitrogen Corporation) at 37 °C in 5% CO_2 in humidified atmosphere. The media were replaced every 3 days. The 80% of confluent cells were subcultured through trypsinization (0.25% trypsin/0.53 M EDTA; In-Vitrogen Corporation). Cells were seeded and cultured on plastic polystyrene (control); titanium plate and HA-coated on ATi at the cell density of 5×10^4 cells/cm^2. Cells were stained using the Live/Dead ®Viability/Cytotoxicity Kit (L-3224, In-Vitrogen Corporation) in a ratio of 2 μM of calcein AM and 4 μM of Ethidium homodimer-1. The fluorescence images from these dyes was observed separately with different filters and investigated by Image J by using upright fluorescence microscope (Olympus AX70, USA).

3. Results and discussion

3.1. Anodized titanium characterization

The XRD pattern (Fig. 2) showed that annealing at 450 °C for 30 min causes transformation of anodized TiO_2 to anatase, body-centered-tetragonal TiO_2. This result is in an agreement with the study by Fang et al. [28,29].

The FE-SEM images (Fig. 3) indicated various morphologies of the TiO_2 prepared by different conditions. Fig. 3a and b shows the irregular array of the nanotubes, which formed in two different electrolytes: NH_4F in 100% H_2O and 10% (NH_4F in H_2O):90% PEG 400. In contrast, the arrays of TiO_2 nanotubes on the titanium substrate, anodized in high viscous electrolyte (10% (NH_4F in H_2O): 90% glycerol) was highly ordered (Fig. 3c). As suggested by Macak et al. [24], high viscous fluid like glycerol suppresses local concentration fluctuations and pH bursts during anodization, which leads to smooth TiO_2 nanotubes, The same phenomenon was also reported by Chanmanee et al. [22] and Marcak and Scimuki [30].

The TiO_2 nanotubes formation mechanism in F^- containing electrolyte is composed of the chemical etching and the enhanced electrical field induced etching of TiO_2 as shown by these reactions:

$$Ti + 2H_2O \rightarrow TiO_2 + 4H^+ + 4e^- \quad (1)$$

$$Ti^{4+} + 6F^- \rightarrow [TiF_6]2^- \quad (2)$$

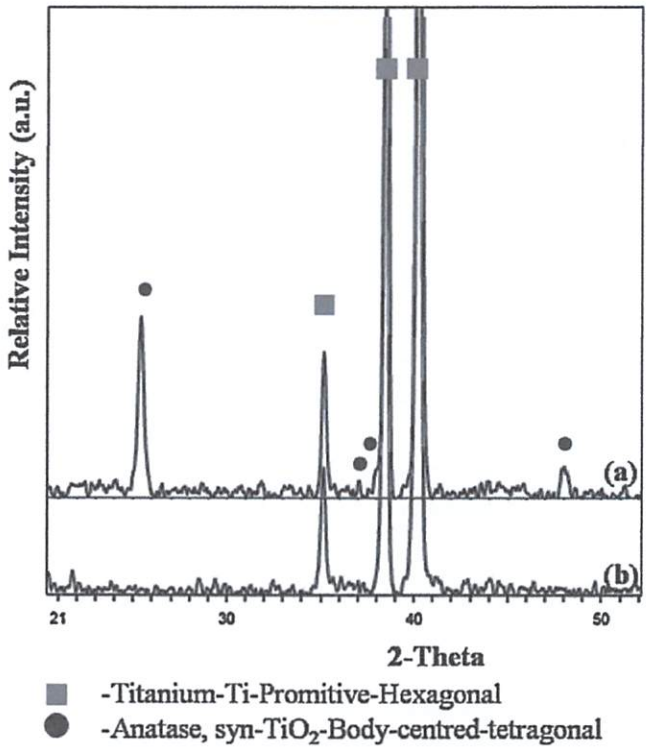

Fig. 2. XRD patterns of titanium oxide obtained by anodization with (a) and without (b) annealing.

$$TiO_2 + 6F^- + 4H^+ \rightarrow [TiF_6]^{2-} + 2H_2O \quad (3)$$

Reaction (1) describes the oxide growth on Ti surface. The fluoride ions in the electrolyte have two roles. First, it reacts with Ti^{4+} ions, which are dissolved at the oxide–electrolyte interface, to form soluble $[TiF_6]^{2-}$ complex (reaction (2)). The other role is to chemically dissolve TiO_2 and then form $[TiF_6]^{2-}$ complex [reaction (3)] [30–32]. As a result of these processes, extensive pores on TiO_2 nanotube, caused by F^- etching, become assembled and become disconnected while reaction (1) still proceeds [33]. This is the self-assembly of TiO_2 nanotube. These reactions, thus, must be carefully balanced in order to form highly-ordered nanotube arrays. It is also found that the highly-ordered TiO_2 nanotube was obtained when pulse anodization was applied (Fig. 4). Importantly, the film morphology is considerably improved when pulse anodization is combined with 90% glycerol as the growth medium. Reactions (1) and (3) occur during positive potential range whereas negative voltage electrostatically induces the binding of NH_4^+ species with TiO_2, as shown in reaction (4), to form adsorbing $TiO_2(NH_4^+)$. The role of $TiO_2(NH_4^+)$ is to protect the nanotube walls against chemical etching by fluoride ions even in a short times of negative potential (1 s) [34–36].

$$TiO_2 + NH^{4+} \rightarrow TiO_2(NH^{4+})ads \quad (4)$$

Effect of anodization time on tube wall thickness, diameter and length of nanotubes were shown in Figs. 5 and 6. The figures suggested that an increase of time significantly increases tube length and decreases wall thickness. The tube lengths of anodized TiO_2 formed for 0.5, 1.5, 2.5 h are approximately 280, 560 and 920 nm, respectively. The wall thicknesses are 12 and 10 nm for anodization time of 1.5 and 2.5 h, respectively. It should be noted that the wall thickness for the nanotube formed at anodization time of 0.5 h is not mentioned here because the shape of nanotube is irregular. The cause of irregularity of TiO_2 layers is because the anodization time is too short. Growth rate at the beginning is much higher than

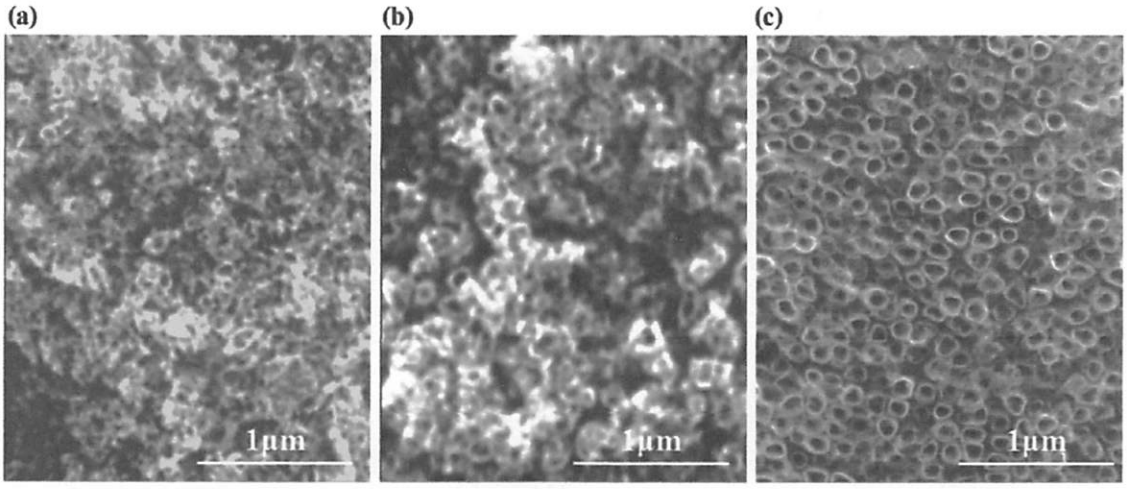

Fig. 3. SEM images of TiO_2 nanotube formed on titanium plates in 0.36 M NH_4F by anodization under different conditions (20 V for 3 h); (a) NH_4F in 100% H_2O; (b) 10% (NH_4F in H_2O):90% PEG 400; and (c) 10% (NH_4F in H_2O):90% Glycerol.

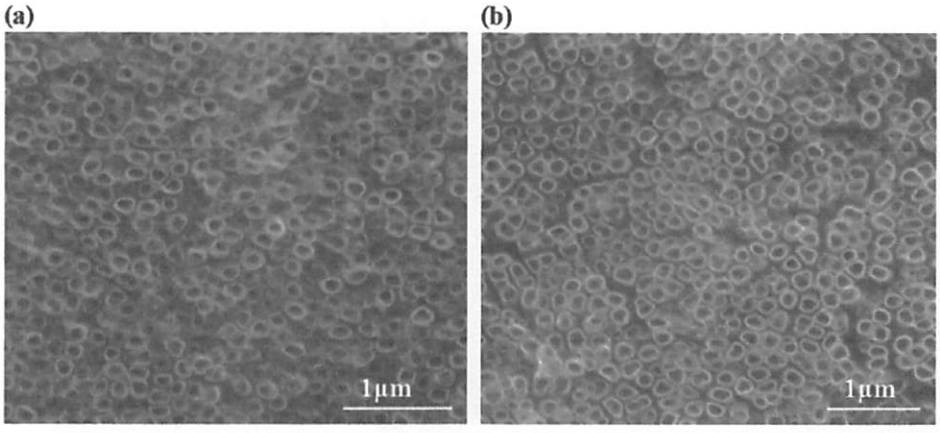

Fig. 4. SEM images of TiO_2 nanotube arrays grown by (a) constant potential anodization (20 V, 3 h) compared with samples grown by (b) pulse anodization at 20/−4 V.

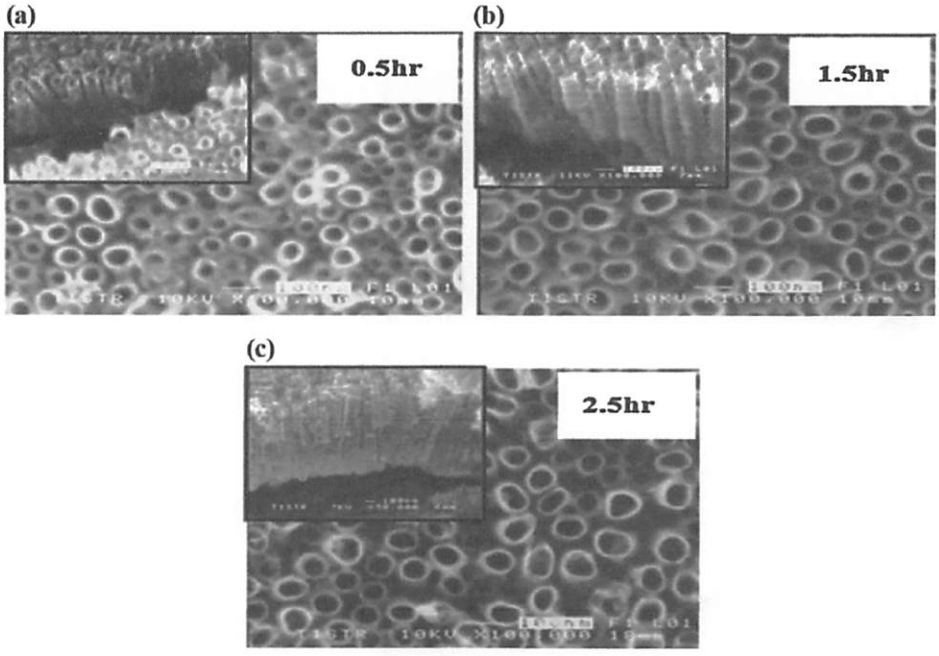

Fig. 5. SEM images of nanotube arrays anodized at various time: (a) 0.5, (b) 1.5 and (c) 2.5 h, which lengths are approximately 280, 560 and 920 nm, respectively. The inner images shows side views of TiO_2 nanotube arrays. All scale bars are 100 nm.

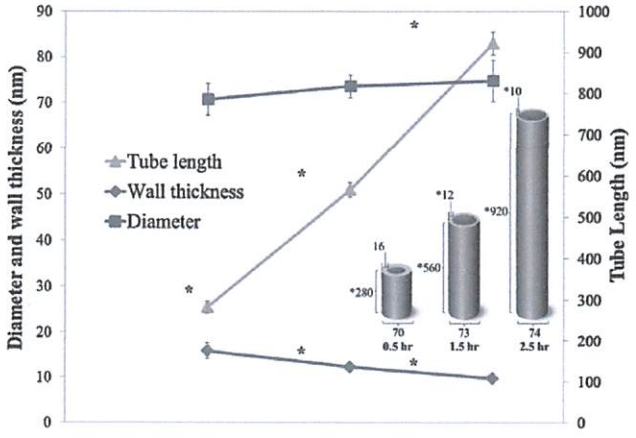

Fig. 6. Wall thickness, diameter and length of nanotubes formed with different anodization times analyzed by Image J. Statistics are calculated using ANOVA. A p-value was calculated using one way ANOVA; $n = 3$, $^*p < 0.05$ when compared with other anodization condition.

dissolution rate because activity of titanium to form oxide layer is still high compared with that of oxide to dissolve in the electrolyte. Consequently, the surface is locally activated and pores start to grow randomly [26]. When anodization time is longer, the individual pores start interfering with each other, and then orderly self-assembly of nanotubes begins to proceed. At this stage, the growth rate is equal to the dissolution rate. Therefore, when anodization time is 1.5 or 2.5 h, the TiO_2 layers were highly order and the structure changes to nanotube form. The difference of nanotube shape may cause different mechanical interlocking between HA coating and nanotube arrays, which will be discussed further in adhesive tape test analysis for HA coated-ATi layers.

3.2. Electrodeposition of hydroxyapatite

EDS result confirmed that the nanostructure of sodium titanate ($Na_2Ti_5O_{11}$ or $Na_2Ti_6O_{13}$) was deposited on the top of the TiO_2 nanotubes, as shown in Fig. 7. The effect of the NaOH pre-treatment on crystal size of electrodeposited HA was previously described by Seung-Han Oh et al. [37]. In that study, after the TiO_2 layers made contact with the NaOH solution, sodium titanate was formed. The sodium titanate enhanced the formation of calcium phosphate during immersion in SBF. The crystal size of HA grown from the sodium titanate surface will be less than the size of that sodium titanate. This mechanism is called "bio-inspired nanostructure". The growth of finer-scale structure of HA from a nanostructured substrate (TiO_2 nanotube arrays) is one way to fabricate nanostructured HA coating

Table 1
Classification of adhesion of the HA coatings to the different anodization times samples and titanium surface.

Substrates for HA coating	Analysis removed area	
	Removed area, %	Category
ATi: 0.5 h	17.75	2
ATi: 1.5 h	2.19	4
ATi: 2.5 h	12.35	3
Titanium plate	98.20	0

for orthopedic implants. However, in their study, sodium titanate was formed at a higher concentration of NaOH compared with this work. The crystal structures of calcium phosphate minerals after grown on both of pretreated-ATi and titanium plate were analyzed by XRD, as shown in Fig. 8. From the figure, HA ($Ca_{10}(PO_4)_6(OH)_2$) coating was found for both of P-ATi and titanium plate, but the higher HA peak were found for the P-ATi substrate.

Fig. 9 shows that HA coating on titanium plate was looser than the coating on ATi. The result was confirmed by tape test. The SEM image of HA coating after tape test was shown in Fig. 10. The image confirmed that adhesion of HA on ATi is better than that of HA on titanium plate. The result is in an agreement with other works, which suggest that using nanotube enhances adhesion between the substrate and the coating [38,39].

3.3. Adhesion of HA coatings on TiO_2 nanotube arrays formed from different times

For the tape test, only some of the HA upper layer is removed and most HA still remains on TiO_2 nanotube layers due to adhesion of the coating on the tube. The area of remaining HA coated-ATi samples after tape test are shown in Fig. 10a–d (OM with SEM image as an inset). Classification results of adhesion of the coatings, evaluated by tape-test, are summarized in Table 1. The removal of the tape from the HA-coated-anodized samples was more difficult than from HA-coated titanium plate samples. Samples without anodization showed large damage area along the cuts after tape test and was classifies as class 0. According to the damage area, samples anodized for 0.5, 1.5 and 2.0 h, were classified as class 2, 4 and 3, respectively. This result indicates that the anodization time of 1.5 h is more suitable than others to be used for preparing the ATi substrate for HA coating.

The better adhesion of HA on ATi than that of HA on titanium plate is probably caused by higher surface area and physical locking between HA coating and ATi. As suggested by Wang et al. [40] TiO_2 nanotube surface promoted mechanical interlocking between HA and TiO_2 nanotube.

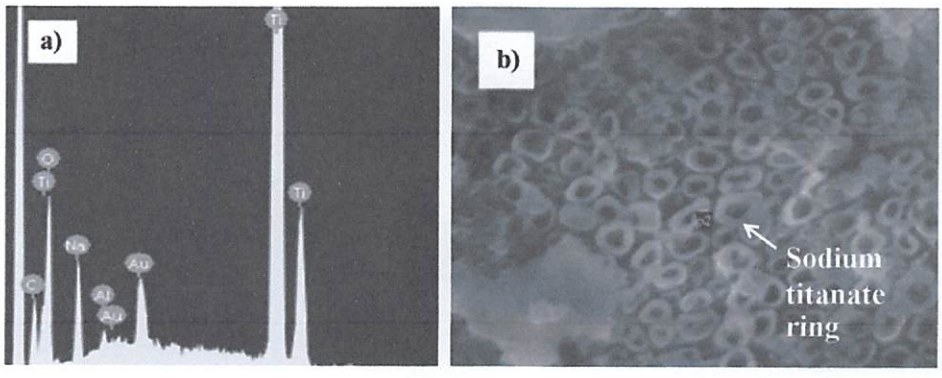

Fig. 7. EDS-SEM analysis of ATi after NaOH pre-treatment: (a) the peaks of elements (Na, Ti and O) and (b) SEM image with the arrows representing TiO_2 nanotube and sodium titanate ring on the top of the nanotube.

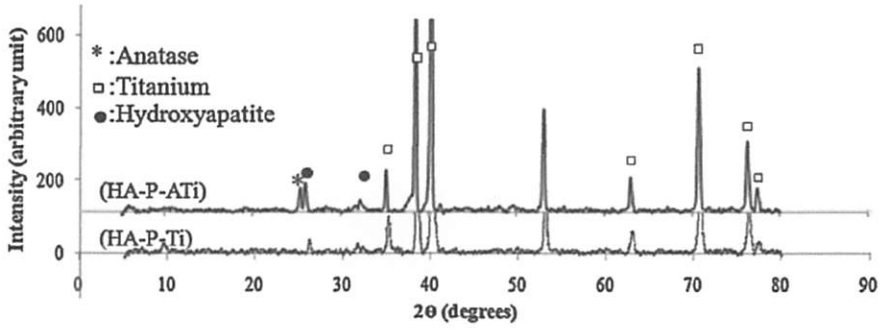

Fig. 8. X-ray diffraction spectra of the electrodeposited HA coatings on titanium plate (HA-P-Ti) and ATi with NaOH pre-treatment (HA-P-ATi).

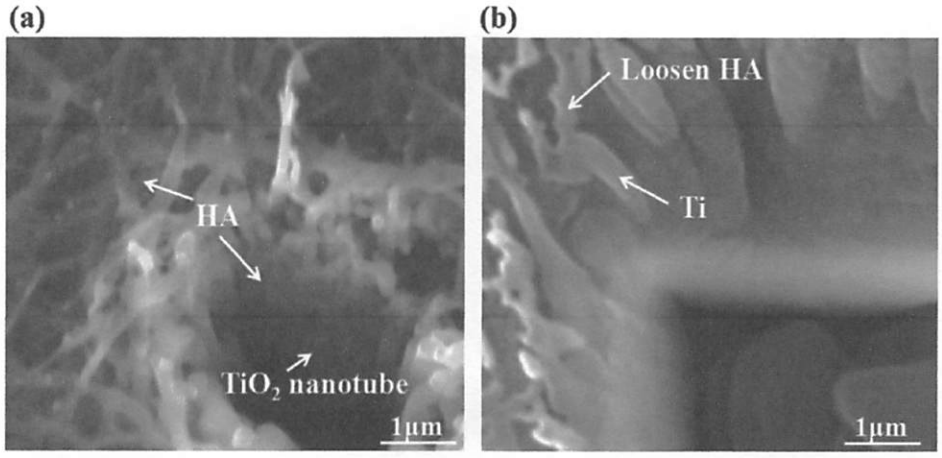

Fig. 9. SEM images of cross-section of HA coating on an anodized titanium (a) and titanium plate (b). Inner images shows surface of each coating.

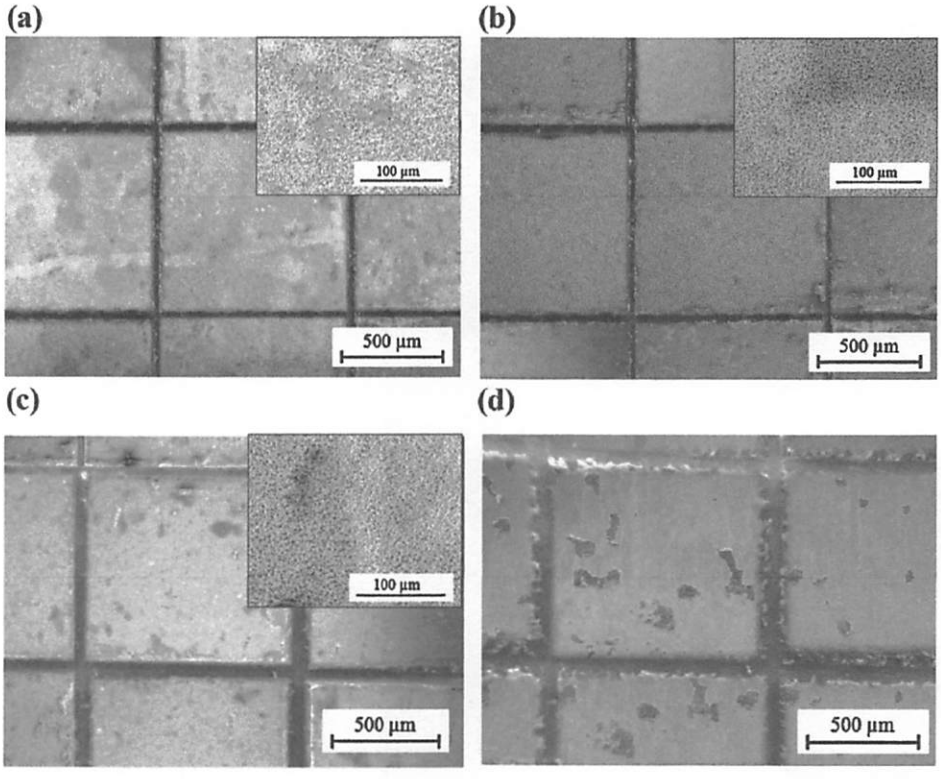

Fig. 10. SEM images shows surface of HA coated on titanium nanotube of different tube length after tape-test: (a) 280 (b) 560 and (c) 920 nm and (d) titanium plate.

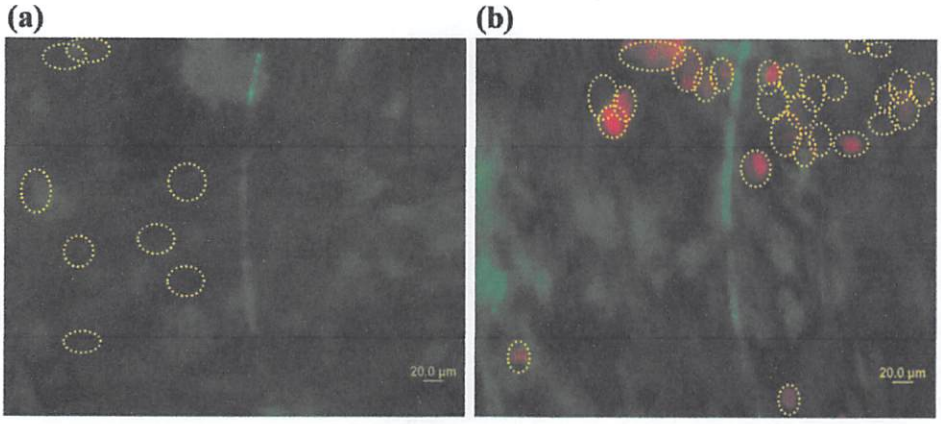

Fig. 11. Live/Dead staining of MC3T3-E1 osteoblasts on HA coated-ATi and HA coated-titanium plate. Dead cells shows in the circle and other cells are the live cells.

In the tape test, axial compressions were induced on TiO_2 nanotube surface. The tube structure could be deformed during tape loading, which induced both collapse and wears of the nanotubes. According to Yokobson et al. [41], the collapse of nanotubes due to axial compression are undergoes various atomistic mechanisms. The explanation for higher damaged surface of HA on tubes with 2.5 h anodization time than that of 1.5 h is due to localized deformation and failure originated by higher nanoscale defects. According to the Euler equation: $\sigma_{cr} = \pi^2 EI/(AL^2)$, the critical stress ($\sigma_{cr}$) that the column can bear is inversely proportional to the second order of the column height, L. The higher the height of the column, the lower is the critical stress that the column can bear. In this study, the height of the column formed for anodization time of 2.5 h is approximately 920 nm which is larger than that of tube anodized for 1.5 h (560 nm). Therefore, the more severe damage was expected for the nanotube anodized for 2.5 h. However, the Euler buckling equation is only valid for long and slender columns loaded axially in compression. For a short column under the axial load, the column will fail by direct compression before it buckles. This failure mechanism might be valid for the 280 nm-height nanotube which formed with anodization time of 0.5 h. In addition to the column height, the tube with larger inner diameter will promote higher adhesion because the HA can grow deeper in the tube pore. As reported previously, the lower the anodization time, the smaller is the tube inner diameter (Fig. 6). Considering both the height and the inner diameter effects, better physical locking between HA coating and the nanotube is expected for 1.5 h-anodized nanotube.

From the morphology and the adhesive tape test, it can be concluded that HA deposition on the nanotube anodized for 1.5 h with NaOH pretreatment is appropriate to be used as biomaterial for further studies.

3.4. Live/dead assay

The vitality of MC3T3-E1 is demonstrated at day 3 by calcein AM/ethidium homodimer-1 staining (Fig. 11a and b). From HA coating on ATi, most cells were alive. In contrast, many of the embedded cells on HA coated on titanium plate were dead, as depicted by red ethidium homodimer-1-stained cells. The osteoblast cell growth were enhanced by HA coated-ATi because HA is better adhered on TiO_2 nanotubes causing a higher number of bone cell growths (the alive cells (greenish cells) were analyzed using Image J) than those cells growth on titanium plate. This result is basically in an agreement with the trend of other works [12,42,43]. Webster et al. shows that overall enhancing bone formation on the implant surface is the relationship of osteoblast adhesion on HA-containing substrates. The preliminary results in the present study indicate that the enhanced osteoblast adhesion and the enhanced nanoscale-HA formation occur simultaneously when using TiO_2 nanotube arrays as a substrate for HA formation and subsequent cell culture. Therefore, the HA coated-ATi that anodized for 1.5 h could be the best choice for a further use in orthopedic applications, because the results suggest that HA coated-ATi can provide a higher number of living cell residence when compared to HA coated on conventional titanium plate. Moreover, HA coated-ATi maintains the highest amount of HA coating on ATi substrates after adhesive tape test in the present study.

4. Conclusion

In summary, TiO_2 nanotubes arrays were successfully fabricated on titanium, which is widely used for orthopedic implants in fluorine-containing anodization. TiO_2 nanotubes were the most highly-ordered when using high viscous electrolyte in anodization with the application of pulse potential. This method is environment friendly, simple and repeatable. Length of the nanotubes could be significantly controlled from about 250 nm to 1 μm. Moreover, at tube length around 560 nm (anodized for 1.5 h) the highest adhesion of HA surface on the nanotube was achieved. TiO_2 nanotube arrays can improve both adhesion of HA on the modified implant and the surrounding bone tissues *in vivo*, which is essential for early bone formation. The Live/Dead cell staining study on anodized titanium, which fabricated from this study, also supports this hypothesis.

Acknowledgement

The authors would like to acknowledge financial support from Commission on Higher Education (the Faculty Development Scholarships) and KMUTT Research Grant. We also thank Asst. Prof. Dr. K. Pasuwat, Mr. C. Manussapol, Mr. C. Jongwanasiri and Ms. K. Siruksasin for their contributions and useful advice in this study; Dr. W. Chanmanee for her advice in anodization; and Ms. W. Chokevivat from National Metal and Materials Technology Center for her help in animal cell experiments.

References

[1] B.D. Boyan, T.W. Hummert, D.D. Dean, Z. Schwartz, Role of material surfaces in regulating bone and cartilage cell response, Biomaterials 17 (1996) 137–146.
[2] X. Zhu, D.W. Son, J.L. Ong, K. Kim, Characterization of hydrothermally treated anodic oxides containing Ca and P on titanium, J. Mater. Sci. Mater. Med. 14 (2003) 629–634.
[3] R.S. Park, J.B. Lakes, Biomaterials: An Introduction, Plenum Press, New York, 1992.

[4] G.E. Chacon, E.A. Stine, P.E. Larsen, F.M. Beck, E.A. McGlumphy, Effect of alendronate on endosseous implant integration: an in vivo study in rabbits, J. Oral Maxillofac. Surg.: Official J. Am. Assoc. Oral Maxillofac. Surg. 64 (2006) 1005–1009.
[5] M. Uchida, H.M. Kim, T. Kokubo, S. Fujibayashi, T. Nakamura, Structural dependence of apatite formation on titania gels in a simulated body fluid, J. Biomed. Mater. Res. 64A (2003).
[6] E. Lugscheider, T. Weber, M. Knepper, F. Vizethum, Production of biocompatible coatings by atmospheric plasma spraying, Mater. Sci. Eng.: A 139 (1991) 45–48.
[7] P. Ducheyne, W. Van Raemdonck, J.C. Heughebaert, M. Heughebaert, A well-adhering Ti-P compound was present at the interface, Biomaterials 7 (1986).
[8] D.R. Cooley, A.F. Van Dellen, J.O. Burgess, A.S. Windeler, The advantages of coated titanium implants prepared by radiofrequency sputtering from hydroxyapatite, J. Prosthet. Dent. 67 (1992) 93–100.
[9] M.C. De Andrade, M.S. Sader, M.R.T. Filgueiras, T. Ogasawara, Microstructure of ceramic coating on titanium surface as a result of hydrothermal treatment, J. Mater. Sci.: Mater. Med. 11 (2000) 751–755.
[10] H.-M. Kim, F. Miyaji, T. Kokubo, T. Nakamura, Preparation of bioactive Ti and its alloys via simple chemical surface treatment, J. Biomed. Mater. Res. 32 (1996) 409–417.
[11] T.J. Webster, C. Ergun, R.H. Doremus, R.W. Siegel, R. Bizios, Specific proteins mediate enhanced osteoblast adhesion on nanophase ceramics, J. Biomed. Mater. Res. 51 (2000) 475–483.
[12] T.J. Webster, L.S. Schadler, R.W. Siegel, R. Bizios, Mechanisms of enhanced osteoblast adhesion on nanophase alumina involve vitronectin, Tissue Eng. 7 (2001) 291–301.
[13] T.W. Chung, D.Z. Liu, S.Y. Wang, S.S. Wang, Enhancement of the growth of human endothelial cells by surface roughness at nanometer scale, Biomaterials 24 (2003) 4655–4661.
[14] T.J. Webster, J.U. Ejiofor, Increased osteoblast adhesion on nanophase metals: Ti, Ti_6Al_4V, and CoCrMo, Biomaterials 25 (2004) 4731–4739.
[15] B.B. Lakshmi, C.J. Patrissi, C.R. Martin, Sol–gel template synthesis of semiconductor oxide micro- and nanostructures, Chem. Mater. 9 (1997) 2544–2550.
[16] Z. Miao, D. Xu, J. Ouyang, G. Guo, X. Zhao, Y. Tang, Electrochemically induced sol–gel preparation of single-crystalline TiO_2 nanowires, Nano Lett. 2 (2002) 717–720.
[17] D. Gong, C.A. Grimes, O.K. Varghese, W. Hu, R.S. Singh, Z. Chen, E.C. Dickey, Titanium oxide nanotube arrays prepared by anodic oxidation, J. Mater. Res. 16 (2001) 3331–3334.
[18] S. Sirivisoot, R.A. Pareta, T.J. Webster, A conductive nanostructured polymer electrodeposited on titanium as a controllable, local drug delivery platform, J. Biomed. Mater. Res. Part A 99 (2011) 586–597.
[19] J.M. Macak, K. Sirotna, P. Schmuki, Self-organized porous titanium oxide prepared in Na_2SO_4/NaF electrolytes, Electrochim. Acta 50 (2005) 3679–3684.
[20] O. Jessensky, F. Muller, U. Göselle, Self-organized formation of hexagonal pore arrays in anodic alumina, Appl. Phys. Lett. 72 (1998).
[21] V. Zwilling, M. Aucouturier, E. Darque-Ceretti, Anodic oxidation of titanium and TA6V alloy in chromic media. An electrochemical approach, Electrochim. Acta 45 (1999) 921–929.
[22] W. Chanmanee, A. Watcharenwong, C.R. Chenthamarakshan, P. Kajitvichyanukul, N.R. de Tacconi, K. Rajeshwar, Formation and characterization of self-organized TiO_2 nanotube arrays by pulse anodization, J. Am. Chem. Soc. 130 (2007) 965–974.
[23] J.M. Macak, H. Tsuchiya, L. Taveira, S. Aldabergerova, P. Schmuki, Smooth anodic TiO_2 nanotubes, Angew. Chem. (Int. ed. in English) 44 (2005) 7463–7465.
[24] J.M. Macak, H. Tsuchiya, L. Taveira, S. Aldabergerova, P. Schmuki, Smooth anodic TiO_2 nanotubes, Angew. Chem. Int. Ed. 44 (2005) 7463–7465.
[25] J. Kunze, L. Müller, J.M. Macak, P. Greil, P. Schmuki, F.A. Müller, Time-dependent growth of biomimetic apatite on anodic TiO_2 nanotubes, Electrochim. Acta 53 (2008) 6995–7003.
[26] A. Kar, K.S. Raja, M. Misra, Electrodeposition of hydroxyapatite onto nanotubular TiO_2 for implant applications, Surf. Coat. Technol. 201 (2006) 3723–3731.
[27] A.S.f.T.a.M. (ASTM), ASTM D3359-02 Standard Test Methods for Measuring Adhesion by Tape Test, 7.
[28] D. Fang, Z. Luo, K. Huang, D.C. Lagoudas, Effect of heat treatment on morphology, crystalline structure and photocatalysis properties of TiO_2 nanotubes on Ti substrate and freestanding membrane, Appl. Surf. Sci. 257 (2011) 6451–6461.
[29] A. Linsebigler, G. Lu, J. Yates, Photocatalysis on TiO_n surfaces: principles, mechanisms, and selected results, Chem. Rev. 95 (1995) 735–758.
[30] G. Balasundaram, T.J. Webster, A perspective on nanophase materials for orthopedic implant applications, J. Mater. Chem. 16 (2006) 3737–3745.
[31] P. Roy, S. Berger, P. Schmuki, TiO_2 nanotubes: synthesis and applications, Angew. Chem. Int. Ed. 50 (2011) 2904–2939.
[32] G.K. Mor, O.K. Varghese, M. Paulose, K. Shankar, C.A. Grimes, A review on highly ordered, vertically oriented TiO_2 nanotube arrays: fabrication, material properties, and solar energy applications, Solar Energy Mater. Solar Cells 90 (2006) 2011–2075.
[33] J.M. Macak, H. Tsuchiya, A. Ghicov, K. Yasuda, R. Hahn, S. Bauer, P. Schmuki, TiO_2 nanotubes: self-organized electrochemical formation, properties and applications, Curr. Opin. Solid State Mater. Sci. 11 (2007) 3–18.
[34] R. Pittman, A. Bell, Raman investigations of NH_3 adsorption on TiO_2, Nb_2O_5, and Nb_2O_5/TiO_2, Catal. Lett. 24 (1994) 1–13.
[35] J. Ahdjoudj, C. Minot, Adsorption of H_2O on metal oxides: a periodic ab-initio investigation, Surf. Sci. 402–404 (1998) 104–109.
[36] W. Chanmanee, A. Watcharenwong, C.R. Chenthamarakshan, P. Kajitvichyanukul, N.R. de Tacconi, K. Rajeshwar, Titania nanotubes from pulse anodization of titanium foils, Electrochem. Commun. 9 (2007) 2145–2149.
[37] S.H. Oh, R.R. Finones, C. Daraio, L.H. Chen, S. Jin, Growth of nano-scale hydroxyapatite using chemically treated titanium oxide nanotubes, Biomaterials 26 (2005) 4938–4943.
[38] K.C. Popat, L. Leoni, C.A. Grimes, T.A. Desai, Influence of engineered titania nanotubular surfaces on bone cells, Biomaterials 28 (2007) 3188–3197.
[39] R.D. Bloebaum, D. Beeks, L.D. Dorr, C.G. Savory, J.A. DuPont, A.A. Hofmann, Complications with hydroxyapatite particulate separation in total hip arthroplasty, Clin. Orthop. Relat. Res. (1994) 19–26.
[40] Y.-q. Wang, J. Tao, L. Wang, P.-t. He, T. Wang, HA coating on titanium with nanotubular anodized TiO_2 intermediate layer via electrochemical deposition, Trans. Nonferrous Metals Soc. China 18 (2008) 631–635.
[41] B.I. Yakobson, M.P. Campbell, C.J. Brabec, J. Bernholc, High strain rate fracture and C-chain unraveling in carbon nanotubes, Computat. Mater. Sci. 8 (1997) 341–348.
[42] T.J. Webster, C. Ergun, R.H. Doremus, R.W. Siegel, R. Bizios, Enhanced functions of osteoblasts on nanophase ceramics, Biomaterials 21 (2000) 1803–1810.
[43] C. Bayram, M. Demirbilek, E. Yalçın, M. Bozkurt, M. Doğan, E.B. Denkbaş, Osteoblast response on co-modified titanium surfaces via anodization and electrospinning, Appl. Surf. Sci. 288 (2014) 143–148.